

LA-UR-13-27010

Approved for public release; distribution is unlimited.

Title: Experimental Investigations – End of Year Technical Report

Author(s): Ulrich, Timothy J. II
Anderson, Brian E.
Le Bas, Pierre-Yves
Payan, Cedric
Reichman, Brent

Intended for: Report

Issued: 2013-09-09



Disclaimer:

Los Alamos National Laboratory, an affirmative action/equal opportunity employer, is operated by the Los Alamos National Security, LLC for the National Nuclear Security Administration of the U.S. Department of Energy under contract DE-AC52-06NA25396. By approving this article, the publisher recognizes that the U.S. Government retains nonexclusive, royalty-free license to publish or reproduce the published form of this contribution, or to allow others to do so, for U.S. Government purposes. Los Alamos National Laboratory requests that the publisher identify this article as work performed under the auspices of the U.S. Department of Energy. Los Alamos National Laboratory strongly supports academic freedom and a researcher's right to publish; as an institution, however, the Laboratory does not endorse the viewpoint of a publication or guarantee its technical correctness.

Experimental Investigations – End of Year Technical Report

Fuel Cycle Research & Development

Prepared for
U.S. Department of Energy
Used Fuel Campaign
T.J. Ulrich, B.E. Anderson, P.-Y. Le
Bas, B. Reichman and C. Payan
Los Alamos National Laboratory
30 August 2013
FCRD-NFST-2013-000XXX



DISCLAIMER

This information was prepared as an account of work sponsored by an agency of the U.S. Government. Neither the U.S. Government nor any agency thereof, nor any of their employees, makes any warranty, expressed or implied, or assumes any legal liability or responsibility for the accuracy, completeness, or usefulness, of any information, apparatus, product, or process disclosed, or represents that its use would not infringe privately owned rights. References herein to any specific commercial product, process, or service by trade name, trade mark, manufacturer, or otherwise, does not necessarily constitute or imply its endorsement, recommendation, or favoring by the U.S. Government or any agency thereof. The views and opinions of authors expressed herein do not necessarily state or reflect those of the U.S. Government or any agency thereof.

SUMMARY

This report summarizes technical work conducted by LANL staff and international collaborators in support of the UFD Storage Experimentation effort. The current focus of this technical work is two-fold: 1) on the detection and imaging of a failure mechanism known as stress corrosion cracking (SCC) in stainless steel (304L) using the nonlinear ultrasonic technique known as TREND, and 2) on the evaluation of concrete integrity in structures with degradation and re-bar corrosion due to carbonation (i.e., CO₂ exposure), also using nonlinear ultrasonic techniques. The latter was performed in conjunction with the Aix-Marseille University and CNRS Mechanics and Acoustics laboratory as part of the French National Research Agency (ANR) EvaDéOs project. The conclusion to be made from these results is that nonlinear ultrasound, in particular TREND, is applicable as a spot inspection technique in both stainless steel and concrete, with the potential to be applied to be more broadly applied to other materials and environments. The nonlinear signature measured is related to the degree of damage/degradation. The localized nature of the measurement allows for identification of mechanical defects and localization of degraded regions. Further work is necessary to characterize the degradation (e.g., sensitivity, size of flaws, type of damage, residual strength, etc.)

CONTENTS

SUMMARY	iv
ACRONYMS	viii
1. INTRODUCTION	1
2. SCC Detection and Imaging	1
2.1 The Time Reversed Elastic Nonlinearity Diagnostic (TREND)	1
2.1.1 Methodology	2
2.1.2 Imaging Crack Orientation	3
2.2 SCC Conclusions and Path Forward	5
3. Inspection of Concrete Structures	5
3.1 Samples	6
3.2 Nonlinear acoustic techniques	6
3.3 Results	6
3.3.1 Nonlinear acoustics	6
3.3.2 Other methods	9
3.4 Crack detection	10
3.5 Path Forward	11
4. References	11

FIGURES

Figure 1. (a) Sample 1: The ROI on the glass-Al plate is shown, outlined by the red box. The delamination in the upper section and the crack running through the middle are clearly visible (b) Sample 2: 304L stainless steel plate with SCC. The ROI is the area around the crack outlined by the green box, with a penny shown for scale. (c) A side view of the ROI in sample 2 showing the apparent angle of the SCC in relation to the surface.	3
Figure 2. (a), (b) and (c) are TREND images developed from the corresponding β values (i.e., nonlinear response determined from SSM) for each orthogonal vector component of motion, X, Y, and Z, respectively. (d) A schematic of the ROI indicating the locations (and approximate size/shape) of the features present (red dashed line indicates the crack in the glass; yellow triangle illustrates the delamination region at the glass-Al interface.)	4
Figure 3. A typical SCC crack in a steel plate is imaged using 3D-TREND. The crack is clearly visible in the x and z directions, while remaining much less obvious in the y direction. This would indicate that the crack runs parallel to the y plane while at an angle to the x and z planes.	5
Figure 4. Evolution of the nonlinearity as a function of the frequency of excitation for 5 samples using SSM. Samples C1-1-3-A and C1-1-4-A are reference samples. C1-2-A, C1-3-A and C1-4-A are carbonated at 10, 20 and 40 mm depth respectively.	7

Figure 5. Measured nonlinearity gradient as a function of the carbonation depth using SSM and PI as nonlinearity index..... 8

Figure 6. Carbonation within the sample (probed surface is on the right) for different samples. The dashed line represents the limit of investigation to keep the assumption that time reversal focuses energy over half a wavelength. 8

Figure 7. Results of radar measurements by the LMDC of the INSA-Toulouse. a) radar amplitude b) Radar speed 9

Figure 8. Concrete resistivity as a function of carbonation depth..... 10

Figure 9. Crack detection using SSM. At each point of the image, wave energy is focused using time reversal and the local nonlinearity is quantified using SSM. The crack shows up as a zone of high nonlinearity. 10

ACRONYMS

AAR	Alkali Aggregate Reaction
ANR	National Research Agency (France)
ASTM	American Society for Testing and Materials
CNRS	Centre National de la Recherche Scientifique (France)
DAE(T)	Dynamic Acousto-Elasticity (Technique)
EES-17	Geophysics Group at LANL
EMPA	Eidgenössische Materialprüfungs- und Forschungsanstalt (Swiss Federal Laboratory for Materials Science and Technology)
ETH	Eidgenössische Technische Hochschule (Swiss Federal Institute of Technology, Zurich)
FCT	Fuel Cycle Technologies
GPR	Ground Penetrating Radar
LANL	Los Alamos National Laboratory
LANSCE	Los Alamos Neutron Science Center
LCND	Laboratoire de Caractérisation Non Destructive (Nondestructive Characterization Laboratory, Aix-en -Provence, France), now part of the LMA
LMA	Laboratoire de Mécanique et d'Acoustique (Laboratory of Mechanics and Acoustics, Marseille, France)
MST-6	Metallurgy Group at LANL
NEWS	Nonlinear Elastic Wave Spectroscopy
NLUT	Nonlinear Ultrasonic Techniques
NRUS	Nonlinear Resonant Ultrasound Spectroscopy
QAPD	Quality Assurance Program Document
ROI	Region of Interest
RUS	Resonant Ultrasound Spectroscopy
SCC	Stress Corrosion Cracking
SPACE	Sub-harmonic Phased Array for Crack Evaluation
TREND	Time Reversal Elastic Nonlinearity Diagnostic
UFD	Used Fuel Disposition

USED FUEL DISPOSITION CAMPAIGN / STORAGE & TRANSPORTATION EXPERIMENTS PROGRAM

1. INTRODUCTION

This document describes the technical work dealing with the determination of the potential for nonlinear elastic wave spectroscopy (NEWS) and other nonlinear ultrasonic techniques (NLUT) to be used for detection, monitoring, characterization and imaging of material degradation in materials relevant to the storage of used nuclear fuel. Particular importance has been placed upon stress corrosion cracking of stainless steel (304L) and various degradation mechanisms of concrete due to the ubiquity of these materials in nuclear fuel storage facilities. We report on two technical efforts, 1) the use of nonlinear ultrasonics for detection and imaging of SCC in 304L, and 2) the application of nonlinear ultrasonics to evaluation of concrete structures for determination of depth of damage penetration and detection of corroded re-bar. This work was carried out at the Los Alamos National Laboratory in accordance with the Fuel Cycle Technologies (FCT) Quality Assurance Program Document (QAPD) and at the Mechanics and Acoustic Laboratory of Aix-Marseille University as part of the EvaDéOs project of ANR.

2. SCC Detection and Imaging

Austenitic stainless steels are known to be susceptible to stress corrosion cracking (SCC), which is an aggressive type of corrosion that exists when a material under tensile stress is placed in a corrosive environment. This is of particular concern as the processing (i.e., cold rolling) and construction (welding) of storage canisters produce an inherent residual stress in metals that can lead to SCC, therefore our goal is to study the formation of stress corrosion cracks within Type 304L stainless steel, which is frequently used in containers for used nuclear fuel disposal. The conditions present in storage canisters (i.e., elevated temperatures, high residual stresses near welds and exposure to salt water/vapor) make them susceptible to SCC potentially leading to critical through-wall failure, and thus loss of containment. The timescales on which through-wall failure has been seen under atmospheric conditions in similar components (e.g., PWR components) is on the order of 10's of years.¹ While through-wall flaws are catastrophic, the long timescales allow for routine inspection, and potentially mitigation, providing methods exist. The following study is focused on the former problem, i.e. detection of SCC, and thus the development of a tool for inspection of storage canisters.

2.1 The Time Reversed Elastic Nonlinearity Diagnostic (TREND)

Time reversal (TR) is a method that allows one to focus wave energy to a specific location in space.²⁻³ Because a TR focus creates a highly localized focus of energy, it can be used to interrogate the nonlinear properties of a specific location in space, where the nearby regions are at lower energy levels. When closed cracks and cracks with small openings vibrate they do so nonlinearly, meaning they exhibit vibration distortions creating signals at new frequencies not present in the source of the excitation (e.g., ultrasonic probe). Open cracks are considered voids and thus respond linearly, or without the aforementioned distortions.⁴ Detecting nonlinearities is easier at higher amplitudes because frequencies of interest (e.g. harmonic frequencies, and sum and difference frequencies, etc.) usually grow as the square of (or higher power than) the fundamental frequency. The time reversed elastic nonlinearity diagnostic (TREND) is a protocol where one creates a TR focus at several locations within a region of interest (ROI). TREND has been used to image surficial and near-surficial nonlinear features in solid samples.⁵⁻⁶

Various physics based techniques can be used to quantify the nonlinearity at each point in a ROI and thus allow crack localization and potentially characterization. The scaling subtraction method (SSM) is one such technique that may be used in a time reversal experiment by creating a low amplitude TR focus and

a high amplitude TR focus at a specific location of interest, scaling the low amplitude signal, and then subtracting the scaled low amplitude signal from the high amplitude signal and integrating the squared signal over a certain time window.⁷

Three-component time reversal focusing has been shown to provide an independent focus of energy in three orthogonal directions on the surface of a solid sample.⁸ Because a TR focus can be independently created in the out-of-plane and both in-plane directions, the nonlinear properties in each of these three independent orientations should be able to be determined using the TREND and the SSM. This report will cover three different sets of experiments where three-component TREND (3D-TREND) is used to image nonlinearities, i.e. crack orientation, in three orthogonal directions on the surface of a sample.

Experiments conducted on two different samples will be presented in this report. One of the samples is an engineered sample used for proof of concept and consists of a cracked glass plate partially glued onto an aluminum plate. 3D-TREND is then used to show that it yields more information about the nonlinear features (a crack and a delamination) than linear imaging can. The other sample is a circular steel plate that has been subjected to magnesium chloride and to significant stress loading in order to induce stress corrosion cracking. A particular significant crack in this sample is then studied using 3D-TREND to image the orientation of the crack.

2.1.1 Methodology

In a TREND experiment with multiple transducers, each transducer in turn emits a source signal, either a pulse or a chirp. A laser vibrometer (LV), either out-of-plane or in-plane, measures the velocity of the motion at a specific point on the surface of the plate. The pulse travels along a direct path to the receiver and along any number of other paths with many internal reflections. Each of the signals measured by the LV is then reversed and sent back through their respective transducers, producing a focus of energy at the receiver position (the time reversal process). This process is repeated with multiple amplitude steps. These amplitude steps can be compared to quantify the amount of nonlinearity present at that point. If the point is linear, an increase in the source strength by N will increase the focal signal by the same amount. If you subtract a scaled lower amplitude step from a higher amplitude step at a linear point (e.g., undamaged material), the residual should be identically zero, though due to noise present in a real-world measurement will be non-zero, though small. At a nonlinear point (e.g., a crack), however, a greater amplitude source signal will introduce higher-order harmonics and phase changes. These changes result in a larger residual. By summing over the original pulse width, these residuals can be compared point by point. This process is called the scaling subtraction method (SSM) and the quantification of the nonlinearity is referred to as β .⁷ Note that this β is not the same as the traditional nonlinearity parameter in nonlinear acoustics. Specifically, the sum of the squared amplitudes over a selected period of time constitutes the SSM residual signal

$$b_i = \frac{1}{T} \int_{t_1}^{t_2} \left(\frac{A_H}{A_L} u_{L,i} - u_{H,i} \right)^2 dt \quad (1)$$

where β_i is the SSM residual metric in the i^{th} direction of velocity focusing, T is the total time over which the integration takes place, t_1 is the start time for the integral, t_2 is the end time for the integral, $u_{H,i}$ is the high amplitude velocity signal in the i^{th} direction of focusing, $u_{L,i}$ is the low amplitude velocity signal in the i^{th} direction of focusing, A_H is the high amplitude value, and A_L is the low amplitude value.

In a 3D-TREND experiment, a full TR experiment is conducted at each point in a grid, and at multiple amplitude levels. The process is repeated independently for each of the three orthogonal components of motion: out-of-plane (Z) and two in-plane directions (X & Y). SSM is then used to produce an image of

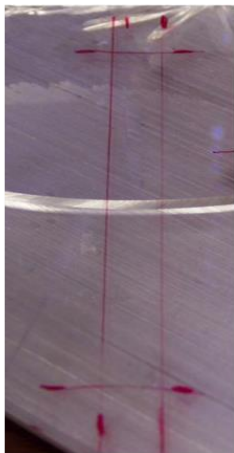
the residual nonlinearity, β , at each point for each of the three components in order to obtain information about the orientation of the crack. For convenience, all TREND images shown in this report use the standard right-handed Cartesian orientation of X, Y, and Z.

2.1.2 Imaging Crack Orientation

The first sample was made to have two different orientations of nonlinear features present. A square glass plate was glued onto a square aluminum plate, both 1/8" thick and 6" by 6". The glue was omitted in certain areas between the two plates to produce delaminations. The glass was then cracked, through an impact applied to the glass, so that the crack and the delamination could be studied together. The bonded plate was then attached to an aluminum block with 1/2" transducers attached. These transducers were used to focus energy at points within the ROI on the bonded plate using TR. A photo of the sample, including the ROI, is shown in fig. 1(a).

The second sample, i.e., the sample containing SCC, is the metal plate shown in fig. 1 (b) and (c). This plate was exposed to magnesium chloride at 150°C for 85 hours and to significant stress loading (the exact stress history was unknown as the sample was made by G.E.) in order to induce SCC. 3D-TREND was then performed on a section with a significant crack in order to understand the orientation of the crack.

(a) Sample 1:
Aluminum
& Glass



(b) Sample 2:
304L Stainless Steel
with SCC



(c) Sample 2:
Sideview
of ROI



Figure 1. (a) Sample 1: The ROI on the glass-Al plate is shown, outlined by the red box. The delamination in the upper section and the crack running through the middle are clearly visible (b) Sample 2: 304L stainless steel plate with SCC. The ROI is the area around the crack outlined by the green box, with a penny shown for scale. (c) A side view of the ROI in sample 2 showing the apparent angle of the SCC in relation to the surface.

In fig. 2 are TREND images constructed from the β values obtained using each component in sample 1. Figure 2(a) shows the residual nonlinearity when TREND is performed using the in-plane X-component, (b) results using the in-plane Y-component, and (c) from the out-of-plane Z-component. Figure 2(d) illustrates the approximate locations and sizes of the mechanical defects as reference for the other images. In the middle of the scan area is the crack. Because this crack is oriented in the X-Z plane, it is not visible in the scans where ultrasonic energy is focused along those components, i.e., parallel to the crack. Fortunately, using a component that is perpendicular to the feature, in this case the Y-component, the crack is clearly visible. The delamination in the upper section of the scan area is also visible, and 3D-TREND gives us information about this as well. Because the delamination is in the X-Y plane (in between

the glass and aluminum plates), the excitations in the X and Y directions do not excite this feature in a manner that a nonlinear response can be generated. However, when TREND is performed using the Z -component, the delamination is visible. In both cases the generation of a nonlinear response only occurs when the probing component is perpendicular to the feature being probed. From this proof of concept experiment we have shown that we can extract two pieces of information: 1) that the dominant mechanism for the nonlinear response is clapping of the unbonded surfaces (because the perpendicular component images the damage); and 2) it is possible to determine defect orientation by inspecting with all three components.

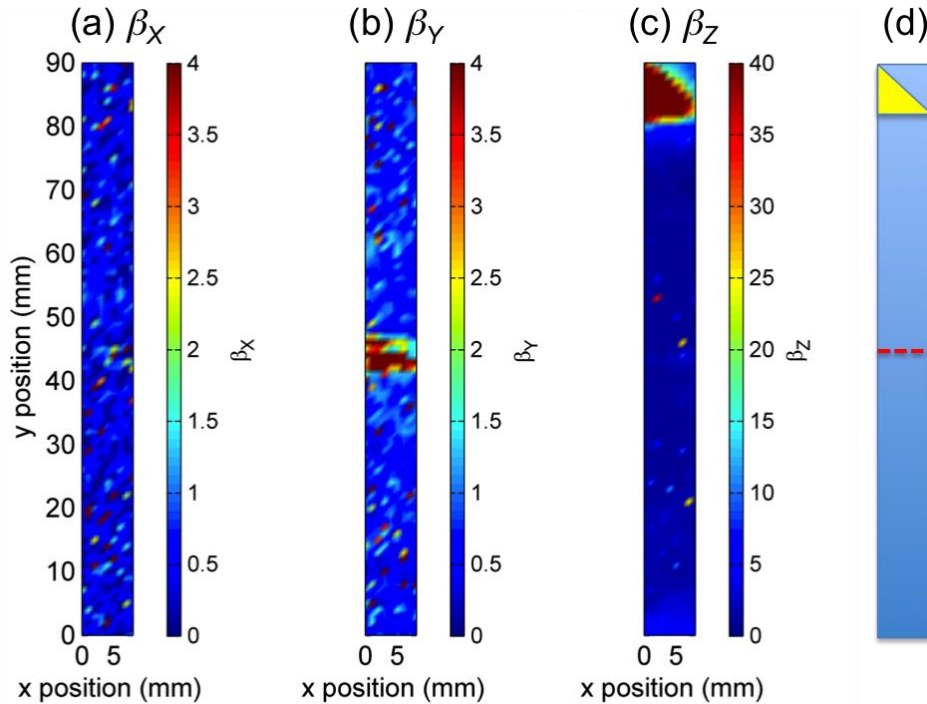


Figure 2. (a), (b) and (c) are TREND images developed from the corresponding β values (i.e., nonlinear response determined from SSM) for each orthogonal vector component of motion, X , Y , and Z , respectively. (d) A schematic of the ROI indicating the locations (and approximate size/shape) of the features present (red dashed line indicates the crack in the glass; yellow triangle illustrates the delamination region at the glass-Al interface.)

The results from the stainless steel plate confirm the ideas presented from the glass-aluminum plate. The different scans again reveal more details about the crack orientation. In the y direction, the crack is not as visible as in the x and z directions. This would indicate that the crack is parallel to the y direction and at a diagonal with both the x and z directions. An examination of the part of the crack visible on the surface and edges of the plate shows that it does indeed penetrate into the material in the x - z direction, as can be seen in fig. 1(b) and (c).

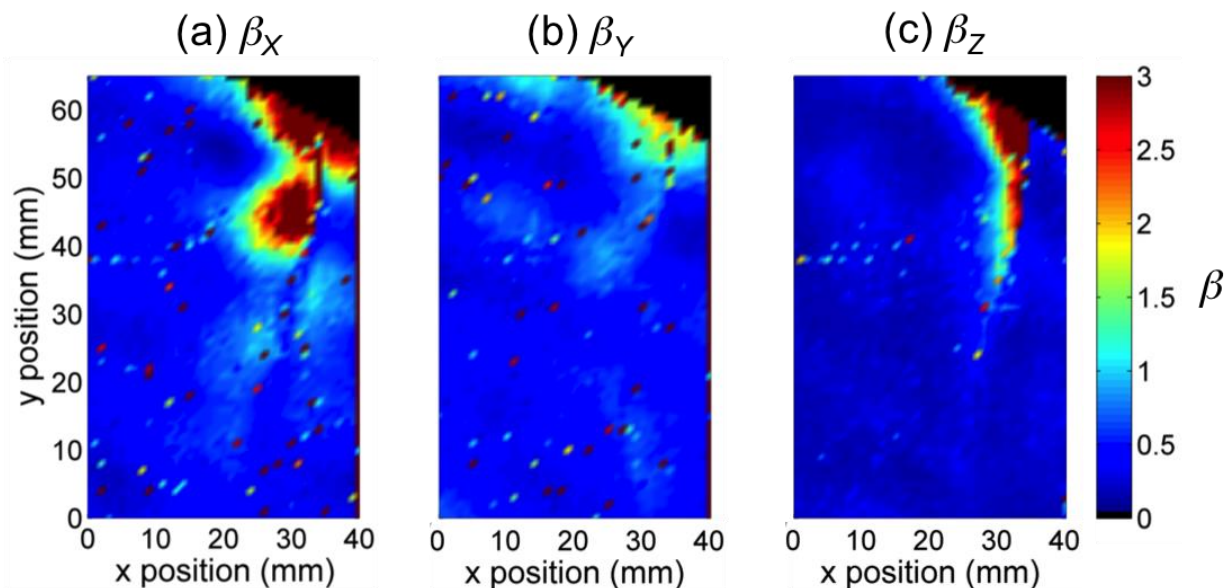


Figure 3. A typical SCC crack in a steel plate is imaged using 3D-TREND. The crack is clearly visible in the x and z directions, while remaining much less obvious in the y direction. This would indicate that the crack runs parallel to the y plane while at an angle to the x and z planes.

2.2 SCC Conclusions and Path Forward

Because TR is able to selectively focus energy in a specific orientation, 3D TREND has been able to successfully identify the orientation of cracks and delaminations. In the glass and aluminum plate sample, 3D TREND was able to distinguish between the crack in the glass and the delamination. In the 304L steel plate sample 3D TREND was able to image the crack and provide information about the internal structure and orientation of the crack. To determine exact orientations it is still necessary to develop a method of combining the information obtained from each of the independent components. This will also require other validation imaging techniques, such as X-ray CT.

It is also necessary to continue research to understand the relationship between frequency and the depth to which the focus penetrates. With knowledge of the shape of the focus underneath the surface and the depth to which it penetrates, more information can be gathered about the depth of a nonlinear feature. Exploring 3D TREND with multiple frequencies can open up new possibilities to give us a better picture of the crack as a whole.

3. Inspection of Concrete Structures

Within the frame of collaboration between LANL and the LMA (Laboratory of Mechanics and Acoustics, Marseille, France), LANL has been involved in the EvaDÉOs project. The purpose of this project is to monitor how concrete evolves when subjected to carbon dioxide exposure. The objective is to be able to detect carbonation before it reaches rebar and thus prevent corrosion and the formation of cracks. Several techniques were used: LANL contributed nonlinear acoustic techniques, other groups in Toulouse, France and Aix-en-Provence, France used linear acoustics (primarily surface waves and time of flight methods) and radar. The following is a description of the samples and of the main results of this project available at the time of this report.

3.1 Samples

The samples were 10x25x50cm blocks of porous concrete. The blocks were covered with aluminum foil on all faces but one and enclosed in a chamber filled with 45% CO₂ at 65% ambient humidity. Sample cores were used as controls to evaluate the depth of carbonation and some samples were taken from the chamber when the carbonation front reached 10, 20 and 40mm. In addition, a selection of samples was left untreated. Porous concrete was used for time consideration, more standard concrete is also being carbonated but samples are not yet ready for testing due to the prolonged exposure time required for less porous concrete.

3.2 Nonlinear acoustic techniques

The basis of nonlinear techniques is to look at how a signal gets distorted with the excitation amplitude. For this, we use time reversal, a technique to focus wave energy, to probe a specific location of the sample. Time reversal focuses wave energy over a half wavelength from the surface of the sample, so by varying the frequency, one can study the evolution of nonlinearity with depth. However, the shape of the focus can be deemed to be a half-wavelength only for wavelengths smaller than the smallest dimension of the sample, so there is a limitation to the depths that can be probed.

We used two methods to quantify nonlinearity, the Scaled Subtraction Method (SSM) and the phase inversion (PI). As defined in section 2.1.1, the principle of SSM is to excite the sample at several amplitudes A_{ni} and record the response signals S_n . We then compute the SSM indicator β_{zn} for the out of plane component for each of the A_n amplitudes, using the lowest amplitude as reference. This set of β_{zn} values is then fit using

$$f(\beta_{zn}) = b A_n^c$$

where the amplitude b and exponent c are the parameters of the fit. b is then used as an indicator of nonlinearity.

The phase inversion is based on the same idea, but instead of doing a scaled subtraction, we add the response S_{n+} to one signal and the response S_{n-} to same signal with opposite phase (i.e. multiplied by -1).

$$PI_n = \int (S_{n+} + S_{n-})^2 dt$$

Doing so at several amplitudes gives a dataset that is fitted using a linear fit. The slope of this fit is used as the second nonlinearity index.

3.3 Results

3.3.1 Nonlinear acoustics

Because of the variability of the aggregates' positions and size/shapes between samples, the absolute value of the nonlinearity is not a reliable indicator, but the variation of the nonlinearity with the frequency used for the time reversal (i.e. the depth of investigation) is significant. Figure 1 shows the variation of the nonlinearity with frequency for different samples using SSM. All curves have been shifted so that their minimum value is 0 to enhance the differences between them.

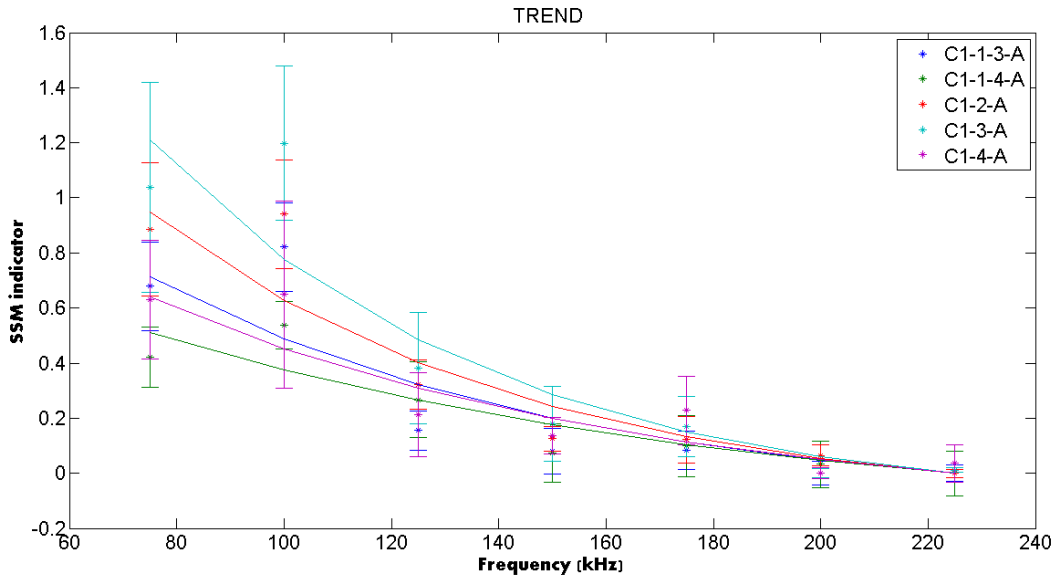


Figure 4. Evolution of the nonlinearity as a function of the frequency of excitation for 5 samples using SSM. Samples C1-1-3-A and C1-1-4-A are reference samples. C1-2-A, C1-3-A and C1-4-A are carbonated at 10, 20 and 40 mm depth respectively.

The curves in fig. 4 show a decrease of nonlinearity when the depth of investigation decreases which is consistent with previous knowledge that nonlinearity decreases with carbonation. Indeed high frequencies means that only the region of the sample close to the surface is probed and this is the most carbonated part of the sample.

To compare samples, we fit each of the curves in fig. 4 with the following formula

$$g(f(\beta_{zn})) = a e^{bf}$$

where amplitude a and exponent b are the fit parameters. We then keep the b to have one value per sample. Physically, this value is an estimation of the gradient of carbonation over the depths of investigation. Figure 5 shows the results for these values using both SSM and PI as quantification of nonlinearity. Both curves have been normalized to the non-carbonated reference value.

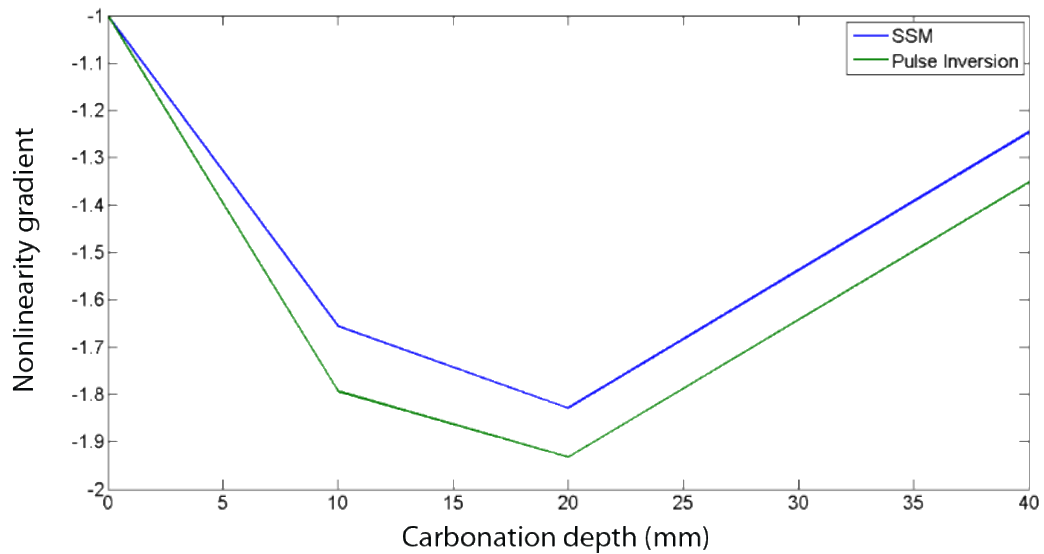


Figure 5. Measured nonlinearity gradient as a function of the carbonation depth using SSM and PI as nonlinearity index.

To explain the evolution of the curves in fig. 5 see the cartoons of fig. 6 representing the carbonation in the sample for each samples.

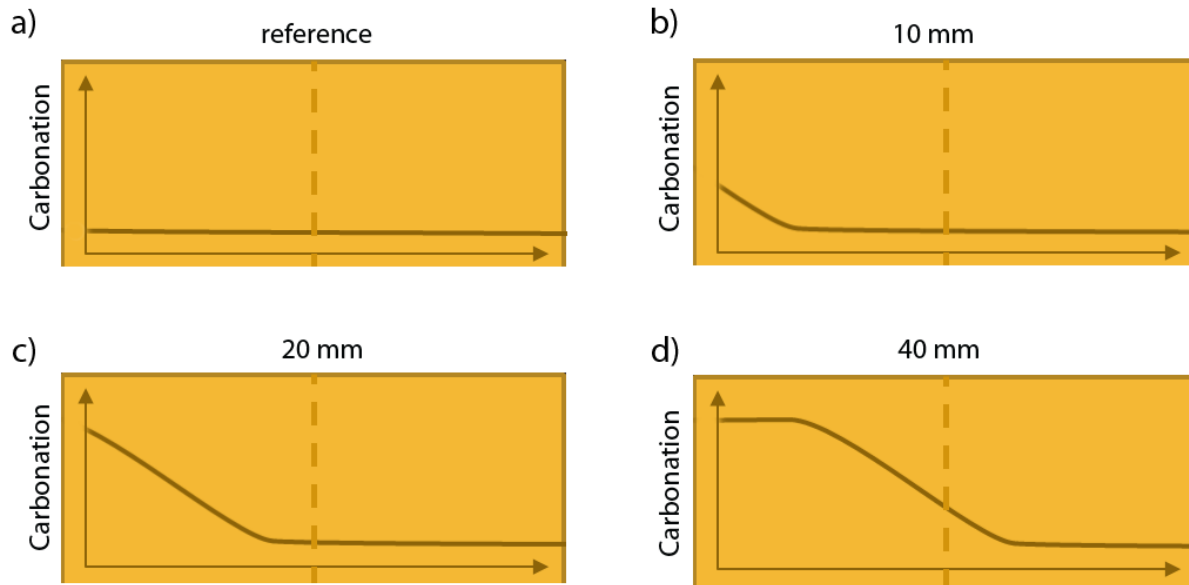


Figure 6. Carbonation within the sample (probed surface is on the right) for different samples. The dashed line represents the limit of investigation to keep the assumption that time reversal focuses energy over half a wavelength.

Figure 6 (b-d) show the progressive increase of carbonation within the sample due to the diffusion of the CO_2 within the samples. This explains that the gradient of nonlinearity is larger (in absolute value) with a larger carbonation depth, as it is the case for the three first points on both curves of Figure 5. Two

phenomena can explain why for a carbonation depth of 40mm the gradient of nonlinearity is lower: the first one is that, 1) there is a saturation of the carbonation reaction when all the chemical elements of the concrete that react with CO₂ have already incurred such a reaction; and the second phenomenon 2) is that if the carbonation front goes beyond our probing limit then the gradient appears to be smaller than it is over the whole thickness of the sample.

To summarize, this study show that nonlinear acoustics allows the detection of carbonation in concrete up to saturation and/or limit of investigation depth. Additional studies are needed to determine how to differentiate between low carbonation and bias results due to the method limitations.

3.3.2 Other methods

Other participants in the EvaDéOS project used other techniques to characterize the carbonation of the samples.

3.3.2.1 Linear acoustics

Measures of the speed of sound and attenuation for longitudinal waves and transversal waves were done. No significant differences were observed between samples carbonated at different depth.

3.3.2.2 Radar measurements

Two measurements were done using radar technology by the Laboratory of Materials and Durability of Constructions (LMDC) of the National Institute of Applied Sciences (INSA) in Toulouse, France.⁹ The preliminary results of those measurements are shown in figure 7.

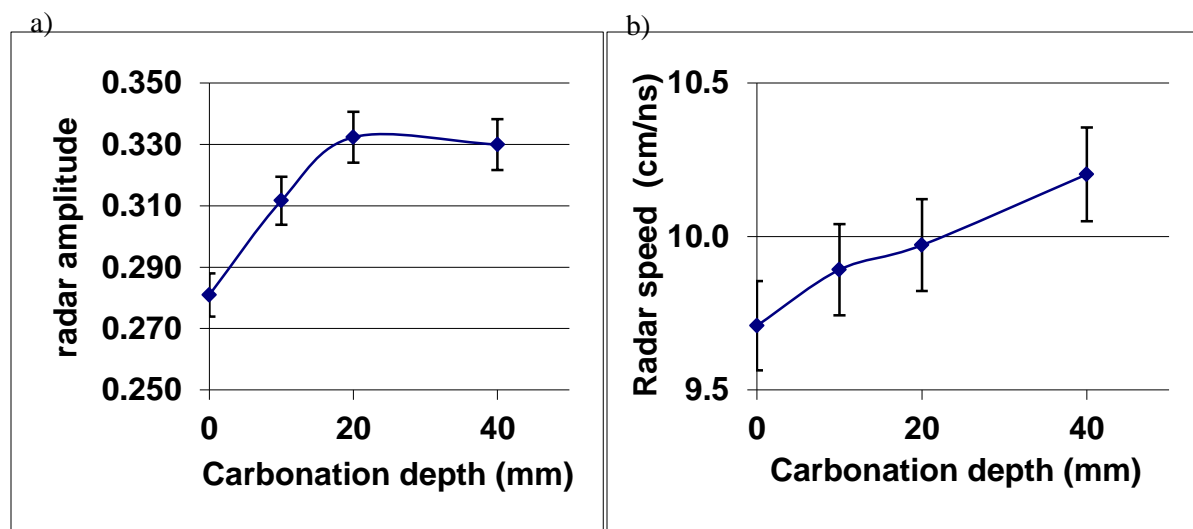


Figure 7. Results of radar measurements by the LMDC of the INSA-Toulouse. a) radar amplitude b) Radar speed

In the case of amplitude, results are similar to the one found with nonlinear acoustics: a strong trend until 20mm carbonation depth and then a plateau or reverse trend. Radar speed measurement seems to give a good correlation with carbonation depth.

3.3.2.3 Resistivity

The LCMD of INSA Toulouse also made some resistivity experiments using the Wenner method.¹⁰ The results are shown in figure 8.

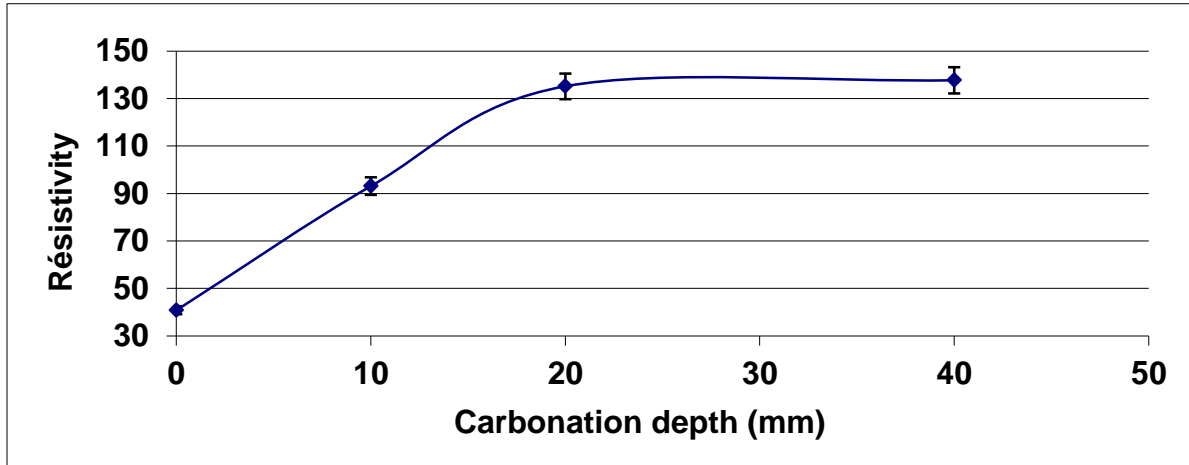


Figure 8. Concrete resistivity as a function of carbonation depth.

Once again, the measurement plateaus at 20mm carbonation depth, which can also be due to the probing depth of the method.

3.4 Crack detection

In addition to detecting carbonation, nonlinear acoustics can be used to detect cracks at their early stage, i.e. at the very beginning of rebar corrosion. Nonlinear acoustics is extremely sensitive to the presence of a crack. By scanning the surface of a sample and looking at the local nonlinearity using the same techniques as describe above (Time Reversal and SSM and/or PI), one can detect cracks as regions of higher nonlinearity as shown in figure 9.

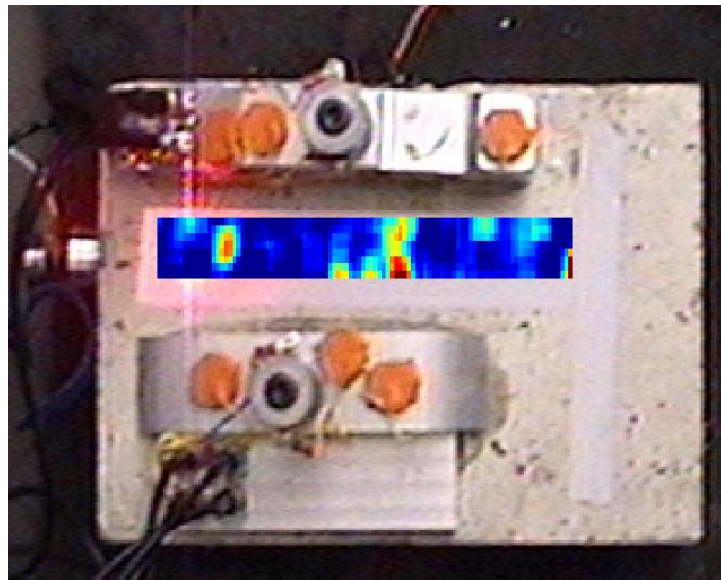


Figure 9. Crack detection using SSM. At each point of the image, wave energy is focused using time reversal and the local nonlinearity is quantified using SSM. The crack shows up as a zone of high nonlinearity denoted by the red points.

It should be noted that cracks due to corrosion will occur after carbonation. As carbonation decreases the natural nonlinearity of concrete, this will enhance the contrast between the background and the crack and facilitate crack detection. As carbonation affects the whole surface exposed to CO_2 , measuring several

points on a surface will still give a measure of the carbonation and not be affected by the presence of local cracks. Both measurements can then be done on the same sample.

3.5 Path Forward

Work still needs to be done to validate the carbonation detection. Ideally, measurements should be done periodically during CO₂ exposure to have a more detailed curve like those shown in fig. 5. There is also a need to discriminate between a low gradient of nonlinearity due to low carbonation and one due to carbonation saturation and limitation of the method in terms of probing depth. Unfortunately, these experiments are not part of the EvaDéOS project and will have to be conducted separately. However, this is a very promising method that could allow for the prevention of rebar corrosion through early detection.

4. References

- 1 J.P. Basson, C. Wicker, Environmentally induced transgranular stress corrosion cracking of 304L stainless steel components at Koeberg, *Proc. Fontevraud 5 Int. Symp. On Contributions of Materials Investigations to Resolution of Problems Encountered in Pressurized Water Reactors*, French Nuclear Energy Society, September 2002.
- 2 M. Fink, Time reversed acoustics, *Phys. Today* **56**, 143–147 (2000).
- 3 B. E. Anderson, M. Griffa, C. Larmat, T. J. Ulrich, and P. A. Johnson, Time reversal, *Acoust. Today* **4** (1), 5-16 (2008).
- 4 Kazakov, V.V., A. Sutin, and P.A. Johnson, “Sensitive imaging of an elastic nonlinear wave source in a solid,” *Appl. Phys. Lett.* 81(4), 646-648 (2002).
- 5 T. J. Ulrich, A. M. Sutin, T. Claytor, P. Papin, P.-Y. Le Bas and J. A. TenCate, The time reversed elastic nonlinearity diagnostic applied to evaluation of diffusion bonds, *J. Applied Phys.* vol. 93, no. 151914, 2008.
- 6 T. J. Ulrich, P. A. Johnson, and A. Sutin, Imaging nonlinear scatterers applying the time reversal mirror, *J. Acoust. Soc. Am.* **119**(3), 1514-1518 (2006).
- 7 M. Scalerandi, A. S. Gliozzi, C. L. E. Bruno, D. Masera, and P. Bocca, A scaling method to enhance detection of a nonlinear elastic response, *Appl. Phys. Lett.* **92** (10), 101912 (2008).
- 8 T. J. Ulrich, K. Van Den Abeele, P.-Y. Le Bas, M. Griffa, B. E. Anderson, and R. A. Guyer, Three component time reversal: Focusing vector components using a scalar source, *J. Appl. Phys.* **106** (11), 113504 (2009).
- 9 G. Klysz and J.-P. Balayssac, Determination of volumetric water content of concrete using ground-penetrating radar, *Cement Concrete Res.* **37** 1164-1171 (2007)
- 10 Z.M. Sbartai, S. Laurens, J. Rhazi, J.P. Balayssac and G. Arliguie, Using radar direct wave for concrete condition assessment: Correlation with electrical resistivity, *J. Appl. Geophys.* **62** 361-374 (2007)